Fast and Reliable Modelling of Offshore Wind Generation for Adequacy Studies

Thuy-hai Nguyen *Student Member, IEEE*, Jean-François Toubeau *Member, IEEE*, Emmanuel De Jaeger *Member, IEEE*, and François Vallée *Member, IEEE*

***Abstract*—Considering the increasing proportion of offshore wind generation in the energy mix, it becomes essential to properly account for aerodynamic effects that impact the power extracted from the wind. Indeed, due to computational constraints, offshore wind energy is currently modelled in a very simple and approximate way in adequacy studies, neglecting important factors such as wake effects. Hence, in this paper, data-driven proxy models are developed for learning the complex relation between free flow wind information and the resulting aggregated output power of wind farms. Those supervised Machine Learning-based models are used as fast and reliable surrogates of wake models, embedding their ability to describe the wind and turbines behavior, but with much lower computational times. These models are then included in an adequacy study built upon sequential Monte-Carlo simulations. The collected results are compared with those obtained with the current simplified modelling approach for offshore generation. We observe the importance of accurately representing intra-farm aerodynamic effects since reliability indices can be significantly underestimated when using the simplified modelling, thus hiding potential stressed conditions within the power system.**

***Index Terms*—Adequacy, Machine Learning, Offshore Wind, VARMA, Wake effects**

I. Introduction

OFFSHORE wind energy is an essential component for a large-scale energy transition: it greatly contributes to our carbon neutral future by generating clean electricity at a price competitive with conventional generation technologies [2]. However, offshore wind is intrinsically intermittent and uncertain. Growing concerns are thus expressed regarding the reliability of future power systems. One part of the power system reliability assessment lies in its adequacy computation, i.e., the evaluation of the long-term ability to cover the load in steady-state conditions. In other words, the power systems adequacy is a way to analyse whether sufficient generation capacity is available to satisfy current and future consumer demand and/or system operational constraints [3]. Such adequacy studies are traditionally carried out by transmission system operators and policy-makers in order to evaluate the risk of generation shortage, thus evaluating the need for investment in additional production technologies. Currently, the most reliable adequacy calculations are performed using a probabilistic iterative method relying on (sequential) Monte-Carlo simulations [4]. This method is easy to implement and thus well suited for large-scale system adequacy evaluation, even though their iterative nature is computationally demanding, which may prevent the use of advanced models to represent the different generation technologies. In particular, the current way of modelling offshore wind generation consists in generating free-flow wind speeds and converting them into power through the use of a single wind turbine power curve. This power output is then multiplied by the number of turbines to assess the global power generated by the wind farm [5]. Such strategies are undermined by the fact that they neglect important factors, such as wind shear, turbulence and wake effects. Those effects, which depend on parameters such as the wind farm (WF) layout or the distance between turbines, clearly influence the aggregated power output, and they must not be disregarded. However, in the current literature, this aspect is either neglected or modeled in a highly simplified fashion through an efficiency coefficient (typically assumed to be equal to around 90% of the nominal WF power [6] or computed using the approximated Jensen velocity deficit wake model [7], [8]). Wake effects, which occur in both onshore and offshore farms, are amplified by the lower ambient turbulence in offshore sea since the wind speed in the wake of a turbine tends to recover more slowly to its initial value [9]. Therefore, wake losses are a major issue for offshore wind farms, which motivates this work of incorporating them into power system adequacy studies. This paper therefore focuses on the consideration of intra-farm aerodynamic effects in offshore wind generation models, which are embedded in sequential Monte-Carlo-based adequacy computations. The challenge is to have accurate wind farm models while avoiding high computational costs. This is achieved by using the recent developments in Machine Learning (ML), which can be used to capture the complex characteristics of wind generation in a fast and reliable way [10]. Modelling offshore wind generation using Machine Learning has already been accomplished in the literature for other applications such as layout optimization, online monitoring or annual energy assessment. In [11]–[13], data (power measurements of individual wind turbines and/or wind information from meteorological masts) are collected at onshore wind farms to develop a Machine Learning based prediction of power produced by each turbine. [11], [12] use neural networks to estimate wind turbine power generation, while [13] makes use of adaptive neuro-fuzzy interference system, cluster center fuzzy logic, k-nearest neighbor and neural networks. While these models exhibit relatively good performance, they rely on measurements, which are rarely available for offshore wind farms. In [14], simulation data of a single wind turbine are used to train regression trees that predict the turbine response for any combination of wind speed, turbulence intensity, and

wind shear that might be expected at a turbine site. However, as one model for each turbine is needed, this method is hardly applicable for large wind farms with numerous turbines. [15] trains two neural networks (wake and turbulence field) with a database built on standalone wind turbine simulations. The developed model is capable of establishing the complex spatial relationship between inflow conditions and the wake fields. However, the power computations for an entire wind farm need the propagation of the wake field, which requires the neural network to be run several times, thus increasing the computation time for large wind farms. In the proposed contribution, to the best of the authors' knowledge, it is the first time that ML-based models are developed with the goal of accurately capturing complex aerodynamic effects while remaining applicable (e.g. computation time) in the context of adequacy computations. Practically, this paper has three main contributions.

Firstly, data-driven proxy models are developed based on supervised ML techniques to improve the representation of offshore wind farms within adequacy tools. However, instead of using measurements, which are inherently limited for newly-installed wind parks and otherwise very difficult to obtain, data are collected using an engineering modelling tool that performs wind farm simulations. The resulting ML models use free-flow wind speed and direction as inputs to generate the output power of the WF. The obtained power is then integrated in Monte-Carlo simulations for adequacy assessment. In this paper, we consider 3 actual Belgian wind farms (with different layouts), each one having its own database and ML model.

Secondly, a new methodology for generating representative yearly time series of correlated wind speeds and wind directions is presented. The procedure is based on vector auto-regressive moving average (VARMA) models, which are able to capture time and space dependencies among dependent uncertain variables. These scenarios are then fed into the ML models to identify the corresponding output power of offshore wind farms.

Thirdly, the scenarios are embedded into an adequacy study, which is performed on a modified IEEE Reliability Test System in order to evaluate the impact of an improved offshore wind generation modelling on adequacy results. Outcomes reveal that gradient boosting trees are efficient in representing the behavior of wind farms, and that the offshore annual energy production is overestimated when neglecting aerodynamic intra-farm effects. As a consequence, it appears that the reliability indices are significantly underestimated by the commonly used approach for offshore generation, which ultimately mislead system operators into believing that the grid adequacy is higher (and thus more favourable) than its true value.

The remainder of this paper is organized as follows. Section II shows how databases are created from wind farm simulations. In section III, several Machine Learning models are presented and compared based on three complementary criteria, i.e., modelling complexity, accuracy and (operational) computational time. Section IV shows how to combine those wind farm models within adequacy studies. A case study is then presented in section V. Finally, main findings and perspectives are summarized in the last section.

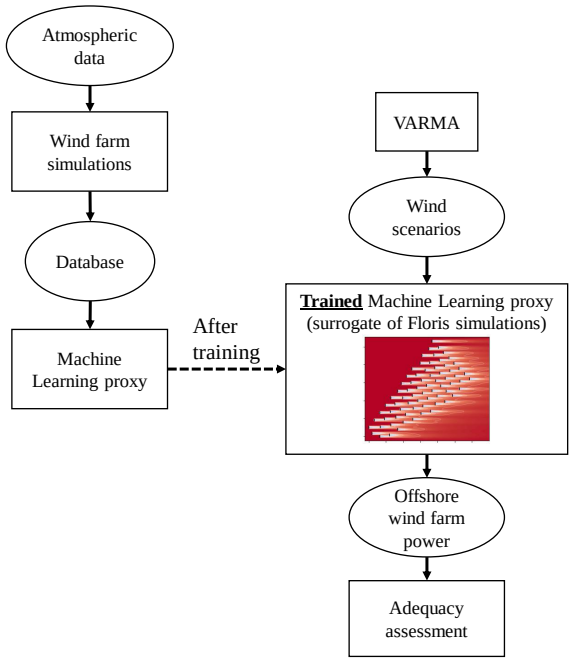

Fig. 1. Methodology scheme to integrate fast and reliable machine learning models of offshore wind generation into adequacy studies.

II. Creation of Database from Wind Farm Simulations

Wind farm simulations (e.g., based on advanced computational fluid dynamics models) cannot be directly integrated in Monte-Carlo simulations wherein millions of simulated power system states are needed to converge towards reliable outcomes. However, a database can be generated from wind farm simulations, which can thereafter be used to train fast Machine Learning models (to be embedded in the Monte-Carlo framework). The methodology is summarized in Fig. 1

A. Floris: a wake modelling engineering tool

For the training stage of those ML models, a database for each wind farm of the power system is created through multiple simulations run with Floris (FLOw Redirection and Induction in Steady state), developed by the National Renewable Energy Lab [16]. This open-source code provides a modeling tool of the steady-state wake characteristics in a wind farm that integrates turbine interactions in wind power plants. Floris implements several wake models: in this study, gaussian models [17] for wake deflection and velocity deficit are chosen. Those models use an analytical solution of the simplified linearized Navier-Stokes equations, which are appropriate for normal turbine operation [18]. Furthermore, different turbulence models are proposed since wake expansion is dependent on ambient turbulence intensity. Here, the Crespo-Hernandez approach is selected for modelling added turbulence arising from turbine operation. Overlapping wakes

are combined using a sum-of-squares approach. In practice, the inputs needed by Floris simulations are the wind farm layout, the wind turbines characteristics (diameter and hub height), and a list of wind speeds and directions. It is assumed that the wind turbine is actively controlled in order to optimize the extracted power without exceeding the maximum allowed power and maximum rotor speed (i.e., maximum power point tracking mode) and that the nacelle is always perfectly aligned with the main wind direction. This is usually called the "greedy" strategy, where each wind turbine is controlled so that its own power is maximized, and it is used in practice in most wind farms [19]. Methods for decreasing wake losses have been proposed in the literature: the main ones being wake steering and axial induction control [20]. However, when used in the context of power maximization, these techniques are associated with an increase on loads and fatigue on the turbine blades [21]. The wind industry has recognized the potential of an improved wind farm control but the actual implementation is still difficult because of the inherent system complexities of wind farms and the aerodynamic interactions among wind turbines. However, if such wind farm controls are to be implemented in the future, it could be taken into account by the proposed surrogate. To that end, new simulations where wind turbines are controlled with yaw steering or induction control could be run, as Floris allows to do so [22].

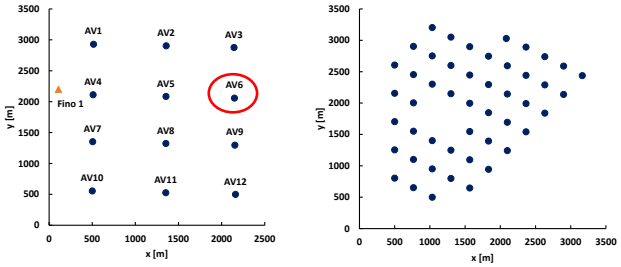

(a) (b)

Fig. 2. Layout of the offshore wind farms used for validation (a) Alpha Ventus, (b) Lillgrund

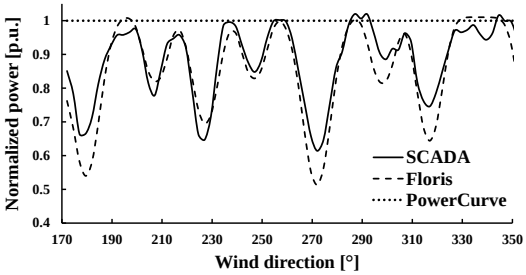

Fig. 3. Comparison of normalized power for a wide sector of wind directions, wind turbine AV6 of the Alpha Ventus wind farm

B. Validation with measurements

In order to validate the utilization of Floris, benchmarks are set up regarding two existing offshore wind farms, for which SCADA (Supervisory Control And Data Acquisition) measurements are available for a limited time period. The output of Floris simulations are compared with the processed SCADA data in terms of normalized power for a given wind speed over a wide range of wind directions. A single turbine is used for the first validation (as individual powers will be the output of the ML model, see section III) while the second validation is for the aggregated power (practically implemented in adequacy studies).

The first validation wind farm is Alpha Ventus, Germany's first offshore wind farm located in the North Sea and built in 2009 [23]. It consists of 12 wind turbines equally spaced, for a total capacity of 60 MW. Measurements have been collected in the scope of the "Research at Alpha Ventus" project (RAVE), which provides data from a multitude of sensors since 2009. In particular, the 100-m-high measuring meteo mast Fino 1 is located directly alongside the wind farm, allowing to record meteorological data such as wind data. Times series from 2011 to 2014 of wind speeds and wind directions from Fino 1 as well as SCADA measurements of electrical power output for one wind turbine were used as a reference for benchmarking. The chosen wind turbine for the validation process is the AV6 turbine (see the Alpha Ventus layout of Fig. 2a). The measurements were pre-processed and filtered before being used to assess the accuracy of the Floris simulations. The normalized power for the wind turbine is plotted against the wind direction, for a wind speed between 9 and 10 m/s and the wind sector [170° - 350°] (where the mast is not waked by the wind farm). It can be seen in Fig. 3 that the Floris simulations (dashed curve) exhibit a good fit with respect to the measurements (full curve): they are able to predict the width and depth of the power deficits. The mean absolute error is 4.62% and the maximum error reaches 13.17%. The slight discrepancies could be explained not only by Floris modelling inaccuracies, but also by measurement noise. The power curve approach does not consider wake effects and the power output of the wind turbine is constant for a given wind speed, independently of the wind direction. For the power curve method, the maximum absolute error reaches 38.61% in full-wake conditions, and the mean absolute error is 11.93%. This clearly emphasizes the limitations of such an approach.

The second validation farm is the Lillgrund offshore wind farm, located near the coast of Sweden. It has a total rated capacity of 110 MW and consists of 48 pitch-controlled, variable speed wind turbines. The layout of the wind farm is presented in Fig. 2b. The SCADA data were extracted from the Lillgrund power assessment report [24]. The normalized total power of the entire wind farm is plotted against the wind direction, for a wind speed of 8 m/s. Again, the Floris simulations (dashed curve in Fig. 4) show a good agreement with the measurements (full curve), whereas the power curve approach (straight dotted line) is always overestimating the produced power. Indeed, in the case of Lillgrund, wake effects occur for every wind direction. The absolute error can reach 55% when using the power curve, and the minimum value is 22%. The mean absolute error rises to 35% in the case of the

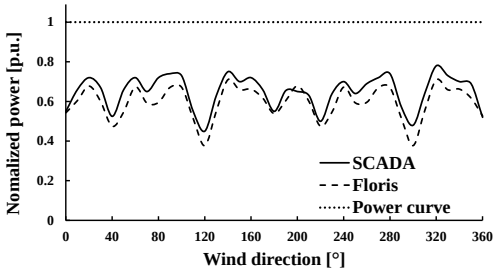

Fig. 4. Comparison of normalized power for a wide sector of wind directions, Lillgrund wind farm

power curve approach, while it only amounts to 5.6% for the Floris computed powers.

Therefore, it can be concluded that Floris simulations offer a good representation of reality when assessing the hourly mean power output of a wind turbine or an entire wind farm.

C. Data generation through wind farm simulations

Three real-life Belgian offshore wind farms (Nobelwind, Norther and Northwind) have been chosen for the database generation. They can be visualized in Fig. 5. For each farm, the layout (wind turbine coordinates) is publicly available on the Royal Belgian Institute of Natural Science website [25] and the wind turbine characteristics are extracted from manufacturers datasheets. As for the list of wind speeds and directions, we use the ERA5 dataset provided by the European Centre for Medium-Range Weather Forecasts (ECMWF) [26]. ERA5 uses reanalysis to generate atmospheric time series covering the period from 1959 to 2021, with an hourly temporal resolution and a spatial resolution of 31 km. Reanalysis combines model data with observations from across the world into a globally complete and consistent dataset using the laws of physics. It provides a comprehensive description of the observed climate as it has evolved during recent decades, on 3D grids at sub-daily intervals. For each wind farm, 3 years of wind (2019 to 2021) as well as extreme scenarios (very high wind speeds) at the location of the offshore wind farms were used as atmospheric input. Hence, a total of 26,311 simulations per wind farm were run with Floris. Interestingly, the resulting database consists not only in the power output of the entire wind farm for a given set of wind speed and direction, but also integrates individual wind turbine power outputs.

Moreover, Floris also allows to run simulations with the option to ignore aerodynamic losses. This method is thus equivalent to the traditional way of modelling wind farms in adequacy studies, where a simple aggregated power curve is used to match free-flow wind speeds to the power output. It is then possible to assess the wake losses, by comparing the annual energy generation with and without taking into account wake effects. This comparison is presented in Table I, where the mean annual energy is computed and averaged for the years 2019-2021 of the ERA5 dataset. It can be seen that although wake losses are similar for the wind farms Nobelwind and Norther (around 7.5-8%), they are significantly higher (15.4%) for Northwind. This can be explained by the different layout and distances between wind turbines. Indeed, as can be seen in Fig. 5, the layout of Northwind is more compact, thus leading to higher losses as the distance between wind turbines is not large enough to allow for wake recovery. Those results clearly emphasize the need to integrate site-specific aerodynamic effects in the offshore wind generation models used in Monte-Carlo adequacy tools, if one wants to have a reliable estimation of the real contribution of offshore wind farms within power system adequacy.

TABLE I
COMPARISON OF MEAN ANNUAL ENERGY PRODUCTION WITH AND WITHOUT AERODYNAMIC LOSSES, BASED ON FLORIS SIMULATIONS

	Nobelwind	Norther	Northwind
Annual E with wake	0.697 TWh	1.489 TWh	0.87 TWh
Annual E without wake	0.753 TWh	1.62 TWh	1.028 TWh
Wake losses	7.42 %	8.09 %	15.36 %

III. MACHINE LEARNING PROXY

For each wind farm, a data-driven Machine Learning model is developed. It is trained using the database produced by Floris (see section II). The dataset used for the training stage of the Machine Learning models consists of 17,551 data samples from the years 2019 and 2020, along with some extreme scenarios. Each data sample represents an hourly value of wind speed and its associated wind direction, with the corresponding hourly power of all wind turbines within the farm as output. The data are divided into a training set (13,163 samples) used to fit the model, and a validation set (4,388 samples) to select the best hyperparameters. To quantify the performances of the model and assess its ability to generalize, the model is evaluated on an unknown dataset. This test set (8,760 samples) consists of data for the year 2021.

The output of the ML model is defined as the power of a wind turbine. Indeed, if the total wind farm power is directly predicted, it prevents the possibility to consider single wind turbine power outages in Monte-Carlo simulations (see section IV-A2). To avoid having one ML model per wind turbine, cross-series learning is used so to have only one model per wind farm. Cross-learning consists in building a (single) global model from multiple series, which is then able to accurately predict individual ones. It allows for various common patterns observed along related series to be effectively learned [27]. Learning from related series not only allows to obtain cross-series information, but also to multiply the number of data. Moreover, only one model is built for multiple series, allowing to save time and computational costs for model selection and hyperparameters tuning. Practically, each sample consists in the free-flow wind speed and wind direction, as well as the power of one wind turbine within the wind farm. An identifying feature is added to each sample, to relate the wind turbine to the corresponding power. The additional features are the wind turbine coordinates within the wind farm (from a

This article has been accepted for publication in IEEE Transactions on Industry Applications. This is the author's version which has not been fully edited and content may change prior to final publication. Citation information: DOI 10.1109/TIA.2023.3307076

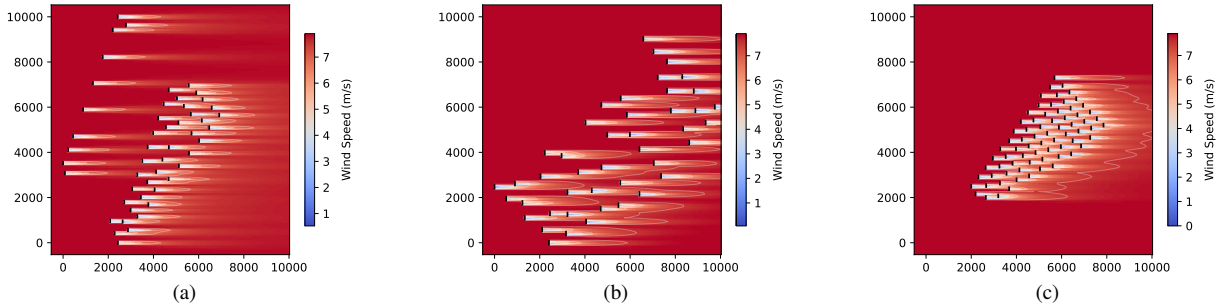

Fig. 5. Floris simulations for a wind speed of 8 m/s and a direction of 270°, for wind farms (a) Nobelwind, (b) Norther and (c) Northwind

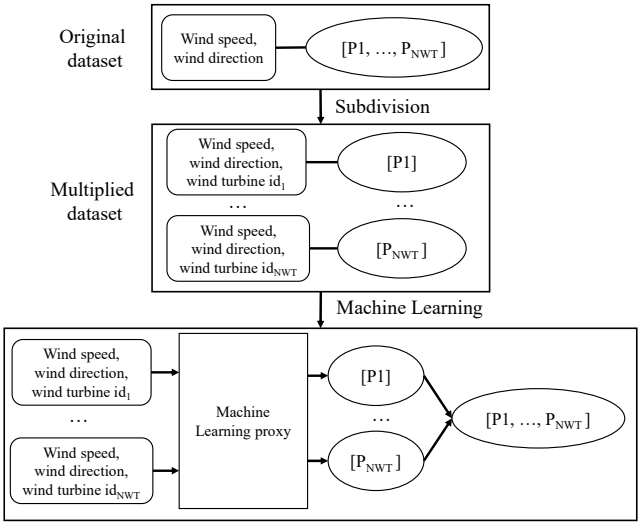

Fig. 6. Cross-series learning: building the new multiplied database

prior conversion in cartesian grid from longitude and latitude information). The number of samples is thus multiplied by NWT (the number of wind turbines within the considered wind farm). The samples are correlated, as the power produced by a wind turbine depends on the wake (and thus the power) generated by the neighbouring turbines. The ML model should be able to learn from these correlations in order to understand the interactions between wind turbines.

For a given set of wind conditions, the powers are predicted one by one, and regrouped afterward to form the total wind farm generation: the process is summarized in Fig. 6

The inputs (features) of the Machine Learning model are thus the wind speed, the wind direction, but also the wind turbine coordinates. The output is the power of the corresponding wind turbine in such wind conditions. The wind farm total power is then obtained by regrouping the single turbine outputs.

The relationship between the wind power output and raw wind information is highly non-linear, which motivates the use of the four following supervised ML algorithms: Decision tree, Random forest, Gradient Boosting Regression Tree (GBRT) and Neural network (more specifically, Multi-layer Perceptron, NN-MLP). Decisions trees can be easily interpreted if their size is reasonable, and they are able to work with features of different scale without a cumbersome data pre-processing. However they tend to overfit and offer thus poor generalization performance. To overcome this problem, multiple decision trees can be combined in order to decrease the variability of the resulting model. Random forests are a collection of independant decision trees, where each tree is built on a random subset of features, using a random sub-sample of the training data set. By averaging the results of all trees, the overall overfitting will be highly reduced. However, random forests performance generally increases with the number of trees in the forest, which inherently increases the computational time and memory requirement. Another ensemble method combining multiple trees is the gradient boosting regression trees algorithm. Unlike random forests, gradient boosting aims at constructing trees in a sequential fashion, where each new tree attempts to rectify the mistakes made by the previous one. As the trees used in this method are not deep, the model needs less memory than random forests. The main drawback of the GBRT method is its high sensitivity to the calibration of hyperparameters, which therefore leads to a complicated fine tuning. The fourth algorithm used in this article involves the use of multi-layer perceptrons (MLP) or feed-forward neural networks. A neural network is composed of several processing units (or neurons), connected to each other by learnable weighted connections with the goal of mathematically representing any relationship between inputs and outputs. Data should be scaled before being used as inputs for a neural network.

The hyperparameters of each algorithm are selected based on a compromise between model complexity, prediction accuracy and computational time [28]. In this study, the model accuracy is assessed using the root mean squared error (RMSE), and the mean absolute error (MAE). RMSE is more sensitive to outliers and penalises large errors, whereas MAE is simply the average of all errors. Lower RMSE and MAE values are associated with more accurate models, and should thus be targeted.

IV. Adequacy Study

Currently, the more accurate adequacy calculations rely on sequential Monte-Carlo simulations. In practice, Monte Carlo simulations can be used to estimate reliability indices

by simulating the actual process and random behavior of the considered electrical system [29]. Sequential simulations allow the use of detailed hourly generation and load models, which makes them ideally suited to the analysis of intermittent generating sources such as offshore wind generation. The principle is to sample successive system states while maintaining the time correlation between consecutive steps. In this work, scenarios of wind speed and direction are generated (and then converted into power using the trained ML models), along with scenarios of load and possible failures of conventional generation units. Overall, the Monte-Carlo sampling process is sequential, i.e., it models all contingencies and operating characteristics inherent to the power system in a chronological time-consistent way.

A. Offshore wind generation

The offshore generation model is composed of two main parts, i.e., the wind model and the wind turbine generator model. These two parts are described as follows.

1) Wind model: Usually, only a wind speed model is needed for adequacy assessment. However, when taking the wake effects into account, the wind direction also has an important influence on the power output of wind turbines. Moreover, when generating wind data, it is important to maintain the correlation between wind speeds and wind directions at different locations. To that end, we use a Vector Auto-Regressive Moving Average (VARMA) model, which augments the ability of ARMA models (that accurately represent time dependencies) with a representation of cross-variables correlations.

In ARMA models, each value in the simulated time series depends on its own lagged values (AR part) but also on current and various past values of a stochastic term (MA part). The model is usually referred to as a ARMA(p, q) model where p and q are respectively the order of the AR and the MA part. First, the series y_t is normalized as follows (to ensure stationarity, as the hourly wind speed distribution is non stationary due to the daily cycle and seasonality) :

$$y_t = \frac{OW_t - \mu_\tau}{\sigma_\tau} \tag{1}$$

where t spans over the dataset, $\tau = t \bmod 8760$, OW_t is the observed wind speed at hour t, μ_τ is the mean of all observed wind speed at hour τ, and σ_τ is the standard deviation of all observed wind speed at hour τ.

Then, the data series y_t can be used to build the following ARMA(p, q) wind speed time series model [30]:

$$\begin{aligned} y_t = {} & \phi_1 * y_{t-1} + \phi_2 * y_{t-2} + ... + \phi_p * y_{t-p} \\ & + \alpha_t - \theta_1 * \alpha_{t-1} - \theta_2 * \alpha_{t-2} - ... - \theta_q * \alpha_{t-q} \end{aligned} \tag{2}$$

where ϕ_i (i = 1, 2, ..., p) and θ_j (j = 1, 2, ..., q) are the auto-regressive and moving average parameters of the model respectively, α_t is a normal white noise process with zero mean and variance σ_a^2, i.e., $\alpha_t \in NID(0, \sigma_a^2)$ with NID denoting Normally Independently Distributed. The maximum likelihood approach is adopted to estimate the values of ϕ_i, θ_j and σ_a^2. A grid search procedure based on the F-criterion is used to determine the order of the ARMA(p, q) model.

Once the wind speed time series model is established, the simulated wind speed can be calculated as:

$$SW_t = \mu_\tau + \sigma_\tau * y_t \tag{3}$$

VARMA(p, q) models for simulating correlated wind speeds and wind directions are just a generalization of ARMA(p, q) models, where the wind speed not only depends on its own lagged values, but also on the lagged values of wind directions. The same goes for the wind direction time series, and the wind vector is written as:

$$\begin{aligned} y_t = {} & \Phi_1 * y_{t-1} + \Phi_2 * y_{t-2} + ... + \Phi_p * y_{t-p} \\ & + \alpha_t - \Theta_1 * \alpha_{t-1} - ... - \Theta_q * \alpha_{t-q} \end{aligned} \tag{4}$$

where $y_t = [y_s, y_w]^t$ contains the data series corresponding to wind speed and wind direction and Φ_i and Θ_j are matrices of dimensions [2x2]. The methodology for estimating the parameters and for choosing the (p, q) order is the same as for ARMA models.

As the goal of the wind model is to generate possible scenarios for future wind data, no wind speed correction is needed (as it would the case for, e.g., forecasting).

2) Wind turbine generator output: A wind turbine is also subject to outages. In order to consider this aspect, the operating cycle of a wind turbine is simulated using a similar procedure as for conventional generation (see section IV-C). In particular, the failures are modelled using a probabilistic model, which provides time steps during which wind turbines are unavailable. For offshore wind turbines, the mean time to failure is 1060 hours and the mean time to repair is 290 hours [31]. It should be noted that several works have been done in order to improve the reliability of wind turbines, e.g., through condition monitoring [32] and fault diagnosis [33]. Enhancing the reliability of offshore wind turbines (i.e., increase the mean time to failure and/or decrease the mean time to repair) would surely lead to an increased power output of offshore wind farms, which in turn would involve a more adequate power system.

B. Load

Since the simulations are sequential, an hourly load profile describing the evolution of load throughout an entire year is needed. This profile incorporates seasonal trends, diurnal cycle as well as weekday/weekend patterns, and is used for all simulated years of the Monte Carlo analysis.

C. Conventional units

Conventional generation units are represented using a two-state model (up state or down state). The up-down-up cycle for a yearly sequence can be generated using a random sampling technique from the corresponding state residence time probability distributions. Here, the time to failure (TTF)

and time to repair (TTR) are assumed to be exponentially distributed and can be computed as follows:

$$TTF = -MTTF * ln\, U \tag{5}$$

$$TTR = -MTTR * ln\, U' \tag{6}$$

where $MTTF$ is the mean time to failure, $MTTR$ is the mean time to repair, U and U' are two uniformly distributed random number sequences between 0 and 1.

D. Sequential Monte-Carlo

The simulation procedure for adequacy assessment is briefly described as follows:

1) Create a model for the availability of conventional generating units using chronological simulations.
2) Construct a model for the wind power output of each wind farm using the time-series VARMA models and the Machine Learning proxies.
3) Compute the total generation capacity of the system (by summing conventional and wind power levels), and compare it with the total load.
4) Compute the reliability indices, which are averaged over all generated scenarios (until convergence is achieved).

This process is carried out on a yearly basis (8,736 hours), and repeated until a specified degree of confidence has been reached. Once the convergence is achieved, the simulation can be terminated. The stopping criterion used in this work is:

$$\frac{\sigma(X)}{\sqrt{N} * E(X)} < \epsilon \tag{7}$$

where X is the reliability index, N is the number of sampling years, $E(X)$ is the mean value, $\sigma(X)$ is the standard deviation and ϵ is a convergence threshold (0.01 in this paper). The reliability indices used in this work are the Loss Of Load Expectation (LOLE) [h/year] and the Loss Of Energy Expectation (LOEE) [MWh/year]. The LOLE is defined as the number of hours in the year during which the electricity consumption exceeds the production, whereas the LOEE computes the energy not served.

V. Numerical results

A. Test case description

The IEEE Reliability Test System (IEEE-RTS) is used for the simulations. The detailed data for the IEEE-RTS are presented in [34]. The base system is modified with the addition of 3 offshore wind farms.

1) Load modelling: The IEEE-RTS chronological load profile consists of 8,736 load points. The annual peak load is 2,850 MW for the IEEE-RTS.

2) Modelling conventional generation: The IEEE-RTS consists of 32 conventional generating units, ranging from 12 MW to 400 MW, with a total capacity of 3,405 MW. The time to failure and time to repair of conventional units are assumed to follow exponential distributions.

TABLE II
Hyperparameters of the ML models

	Nobelwind	Norther	Northwind
	Tree		
Depth	8	6	14
	Random forest		
Number of trees	30	20	30
Depth	8	6	12
	Gradient boosting regression tree		
Number of trees	100	100	120
Depth	6	5	6
Learning rate	0.5	0.4	0.5
	MLP neural network		
Hidden layers	[40, 40]	[30, 30]	[60, 60]
Activation function	tanh	tanh	tanh

3) Modelling offshore wind generation: The IEEE-RTS system is modified with the addition of 3 offshore wind farms, connected to bus 17. Their characteristics are based on existing wind farms in Belgium: Nobelwind (165 MW), Norther (369.6 MW) and Northwind (216 MW), for a total amount of 750.6 MW. The wind database used to construct the VARMA model is the same as the one described in section II (ERA5). For this database, the F-criterion leads to a VARMA(3, 2) model for the generation of correlated wind speed and wind direction time series. It is important to note that it is assumed that the 3 offshore wind farms are totally uncorrelated, and the wind time series are therefore independently produced. While we fully account for intra-farm effects, we suppose that the wind farms are located far enough from each other so that interactions between them can be safely ignored.

B. Performance of Machine Learning models

For each wind farm, the four ML models are trained using the database produced with Floris simulations. After a parametric grid search and a dedicated sensitivity analysis, the hyperparameters selected for each algorithm and each wind farm are presented in Table II.

The performances of each ML model, for each of the three studied wind farms, are given in Table III. The RMSE and MAE are computed on the test set and are given in MW but also in percentage of the wind farm total capacity. The computation times needed by the trained models to predict a yearly power output (8,736 samples) for each wind farm is also presented (inference time). For comparison, the time necessary to produce such an output using Floris simulations is 3775.83 s for Nobelwind, 3121.40 s for Norther and 6449.48 s for Northwind. The enormous difference in computation time between Floris and the ML models clearly proves the relevance of using such ML models as surrogates of wind farm simulations in Monte-Carlo runs, which usually need to simulate hundreds of years to reach convergence.

Every ML algorithm shows strong performance in terms of prediction accuracy and inference time (needed in the

TABLE III
MACHINE LEARNING MODELS PERFORMANCE

	Tree	RF	GBRT	NN-MLP
	Nobelwind			
RMSE [MW]	3.74	3.55	1.17	2.93
RMSE [%]	2.49	2.37	0.78	1.95
MAE [MW]	2.23	2.12	0.73	1.91
MAE [%]	1.49	1.41	0.48	1.27
Inference time [s]	0.06	0.12	0.19	0.54
	Norther			
RMSE [MW]	4.71	4.22	2.02	3.14
RMSE [%]	1.28	1.14	0.55	0.85
MAE [MW]	3.20	2.91	1.49	2.22
MAE [%]	0.86	0.79	0.40	0.60
Inference time [s]	0.04	0.08	0.15	0.39
	Northwind			
RMSE [MW]	5.17	5.66	2.42	5.03
RMSE [%]	2.17	2.38	1.02	2.12
MAE [MW]	2.85	3.28	1.44	3.13
MAE [%]	1.20	1.38	0.60	1.32
Inference time [s]	0.08	0.21	0.26	1.05

Monte Carlo simulations). The decision tree is the fastest algorithm but the accuracy is the lowest. Random forests slightly improve the error metrics, but at the cost of a higher prediction time. GBRT exhibits a promising accuracy and a reasonable inference time. For this algorithm, the RMSE and MAE represent less than 1% of the total wind farm installed capacity. The MLP takes more time to give predictions and is less accurate than GBRT. Based on those observations, a GBRT model is selected to convert the wind speed and direction (generated by the VARMA model) into wind power at each time step of the Monte-Carlo simulations.

C. Impact of aerodynamic losses on adequacy indices

Sequential Monte-Carlo simulations were run using the methodology described in section IV. The wind farms are gradually added to the test system, to assess the influence of an increase of offshore installed capacity. In order to quantify the impacts of disregarding aerodynamic effects, the offshore wind generation is computed using both the GBRT model and the simple aggregated power curve. The results are presented in Table IV. It can be seen that the reliability indices change significantly, depending on how the offshore generation is modelled. With only one wind farm in the system (Norther, 369.6 MW), the difference in reliability indices when incorporating aerodynamic losses is rather low (7.75% for the LOLE and 8.28% for the LOEE). In particular, ignoring the aerodynamic losses caused by wake effects leads to an overestimation of annual offshore energy production of 8.12%. For the power system including two wind farms (Norther and Nobelwind, 534.6 MW in total), the difference increases, meaning that the traditional power curves approach for offshore wind modelling overestimates even more the actual adequacy of the power system. Finally, with 3 wind farms (750.6 MW), the reliability indices further diverge, with a relative difference reaching 35.09% for the LOLE and 37.18% for the LOEE. The annual offshore energy is overestimated by 12.67% when ignoring the wake effects. When the installed offshore generation increases, the annual energy of wind farms (both computed with the ML model and the power curve approach) increases as well, while the reliability indices decrease. Indeed, as the installed generation is enlarged while keeping the load identical, the adequacy of the system is improved. However, while the difference in annual energy increases as well, the difference in reliability indices remains stable. This explains why a 12.67% difference in offshore wind translates into a 35% difference in adequacy indices.

TABLE IV
RELIABILITY INDICES, WIITH OFFSHORE GENERATION COMPUTED WITH ML PROXIES AND POWER CURVES

	LOLE	LOEE	Annual E
With 1 wind farm (Norther)			
ML proxies	3.99 h/year	465.20 MWh/year	1.19 TWh
Power curves	3.71 h/year	429.66 MWh/year	1.30 TWh
Absolute difference	0.29 h/year	35.54 MWh/year	0.11 TWh
Relative difference	7.75 %	8.28 %	8.12 %
With 2 wind farms (Norther and Nobelwind)			
ML proxies	2.49 h/year	262.46 MWh/year	1.76 TWh
Power curves	2.18 h/year	225.90 MWh/year	1.93 TWh
Absolute difference	0.31 h/year	36.56 MWh/year	0.18 TWh
Relative difference	14.05 %	16.22 %	9.12 %
With 3 wind farms (Nobelwind, Norther and Northwind)			
ML proxies	1.31 h/year	139.02 MWh/year	2.46 TWh
Power curves	0.97 h/year	101.97 MWh/year	2.81 TWh
Absolute difference	0.34 h/year	37.05 MWh/year	0.36 TWh
Relative difference	35.09 %	37.18 %	12.67 %

The relative difference in energy with 3 wind farms added to the power system is well aligned with the current literature, where average power losses due to wind turbine wakes are of the order of 10 to 20% of the total power output in large offshore wind farms [35].

Therefore, it becomes clear that modelling the offshore generation in a more accurate way becomes necessary. Otherwise, reliability indices can be significantly underestimated, especially when the number of offshore wind farms, i.e. the installed capacity, increases.

D. Sensibility analysis to the peak load

The peak load, initially 2,850 MW in the IEEE-RTS, is gradually increased to account for the addition of the 3 offshore wind farms. Increasing the load peak value results in the profile load being higher throughout the year. The reliability indices as well as the annual energy production, computed using both the GBRT model and the simple aggregated power curve, are compared. This comparison is made by studying the difference in computed LOLE, LOEE and annual energy when using the ML proxy on the one hand and the power curve method on the other hand. The relative difference in annual offshore energy production remains around 11% to 12%, for annual peak loads varying from 2,850 MW to 3,575 MW.

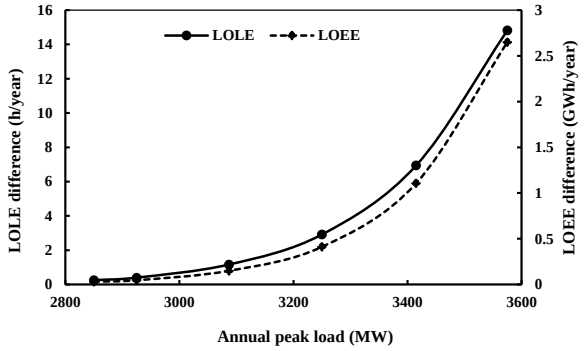

Fig. 7. Difference in reliability indices when annual peak load is increased

TABLE V
RELIABILITY INDICES WHEN ADDING BATTERY STORAGE, WITH OFFSHORE GENERATION FROM ML PROXIES (ML) AND POWER CURVES (PC)

Batteries Power/Capacity	ML proxy		Power curve	
	LOLE [h/y]	LOEE [MWh/y]	LOLE [h/y]	LOEE [MWh/y]
50 MW/150 MWh	0.90	96.05	0.75	80.95
100 MW/300 MWh	0.64	70.17	0.55	70.27
150 MW/450 MWh	0.53	80.65	0.38	58.06
200 MW/600 MWh	0.49	77.48	0.33	52.28
250 MW/750 MWh	0.37	61.88	0.31	52.75
300 MW/900 MWh	0.28	48.26	0.19	30.13

However, it can be seen in Fig. 7 that the difference for both the LOLE and the LOEE increases along with the annual peak load. Indeed, for low values of the annual peak load, the reliability indices mainly depend on the conventional generation scenario because the total conventional generation is high enough to cover the load. In that case, the offshore generation does not have a large influence on the adequacy. However, when the level of consumption increases, the offshore generation becomes then essential to cover the missing power when conventional units are down. It increasingly determines whether or not the total generation is enough to cover the load for the considered power system state. Therefore, in case of important contribution of offshore wind generation in the generation system, it is essential that the losses arising from aerodynamic phenomena are taken into full consideration. Otherwise, reliability indices are underestimated, which may hide important adequacy issues, thereby preventing to take the necessary planning actions to improve the reliability of the system.

E. Addition of energy storage system

Energy Storage Systems (ESS) are often coupled with wind generation, as the intermittency of wind power creates operational uncertainty for power systems [36]. Based on [37], a battery storage device with a maximum charge and discharge rate of 50 MW, a round trip efficiency of 85%, and a usable energy storage capacity of up to 150 MWh (i.e., energy-to-power ratio of 3) has been added to the test system. The device has unbounded ramp rates and no other operational constraints. The storage operation is optimized such that the battery is charged as soon as there is enough production, and discharged during scarcity events. With the Machine Learning model (considering wake effects), the LOLE decreases from 1.31 h/year to 0.90 h/year and the LOEE from 139.02 MWh/year to 96.05 MWh/year. With the power curve approach, the LOLE goes from 0.97 h/year to 0.75 h/year, and the LOEE from 101.97 MWh/year to 80.95 MWh/year. To reach a LOEE target (e.g., 50 MWh/year), the considered battery is duplicated and progressively added to the test system (see TableV). When ignoring wake effects, 150 MW of batteries are enough to reach the arbitrary LOEE target. However, with the Machine Learning model that considers aerodynamic losses, 300 MW of batteries are necessary. This proves that considering wake effects is not only crucial for obtaining more realistic adequacy results, but also to size possible energy storage systems needed to accommodate excessive wind energy. Indeed, ignoring wake effects leads to an overestimation of the produced offshore energy, which in turn involves an under sizing of storage devices.

VI. CONCLUSION

In this paper, a new methodology is presented to model the offshore wind generation in a fast and accurate way, in the context of adequacy assessment. In particular, aerodynamic phenomena arising from wake effects are considered in the power output of wind farms by training a dedicated machine learning model for each wind farm. These models are integrated in sequential Monte-Carlo simulations. The proposed methodology can be applied to any wind farm, even if it is not yet built. Indeed, the methodology requires the knowledge of the layout of wind farm, wind turbine characteristics as well as correlated hourly wind speeds and wind directions, at the location of the wind farm. These data can be easily gathered, as datasets of wind data are widely available as well (as opposed to wind farm output power data) and characteristics of existing wind farms are easily found online.

The results of the test case show that improving the offshore wind energy modelling has a large impact on the reliability indices. Indeed, when compared to our method, the traditional offshore modelling approach, where aerodynamic phenomena are ignored, leads to an underestimation of LOLE and LOEE values. The annual offshore energy production is overestimated by more than 12% when using the traditional approximate modelling. This proves that in the current energy transition context, where offshore wind generation plays an increasing role, it is important to improve the way it is considered when assessing the adequacy of power systems.

As a perspective to this work, one may consider inter-farm effects. Indeed, if the considered wind farms are located close to each other, some wind turbines of one farm could affect the closest wind turbines of a neighboring wind farm. Moreover, the reliability of the medium voltage network that collects power from wind turbines could also be taken into account. Moreover, wind farm control strategies such as wake steering or induction control should be taken into account when these

methods will be implemented by the wind industry. Finally, the optimal configuration of the energy storage system in the case of power systems with a high penetration of offshore wind generation (sizing, type of storage, ...), taking wake effects into account, could be the object of a dedicated study.

ACKNOWLEDGMENTS

ERA5 reanalysis is available from C3S Climate Data Store, see https://doi.org/10.24381/cds.adbb2d47 (C3S, 2017).

Data was made available by the RAVE initiative, which was funded by the German Federal Ministry of Economic Affairs and Energy on the basis of a decision by the German Bundestag and coordinated by Fraunhofer IWES.

This research is supported by the Energy Transition Funds project "PhairywinD" organized by the Belgian FPS economy.

REFERENCES

[1] T.-h. Nguyen, J.-F. Toubeau, E. De Jaeger, and F. Vallée, "Machine learning proxies integrating wake effects in offshore wind generation for adequacy studies," in *2021 IEEE International Conference on Environment and Electrical Engineering and 2021 IEEE Industrial and Commercial Power Systems Europe (EEEIC/I&CPS Europe)*. IEEE, 2021, pp. 1–6.

[2] S. A. Hosseini, J.-F. Toubeau, Z. De Grève, and F. Vallée, "An advanced day-ahead bidding strategy for wind power producers considering confidence level on the real-time reserve provision," *Applied Energy*, vol. 280, p. 115973, 2020.

[3] R. Billinton, R. Karki, Y. Gao, D. Huang, P. Hu, and W. Wangdee, "Adequacy assessment considerations in wind integrated power systems," *IEEE Trans. Power Syst.*, vol. 27, no. 4, pp. 2297–2305, 2012.

[4] A. A. Kadhem, N. I. A. Wahab, I. Aris, J. Jasni, and A. N. Abdalla, "Computational techniques for assessing the reliability and sustainability of electrical power systems: A review," *Renewable and Sustainable Energy Reviews*, vol. 80, pp. 1175–1186, 2017.

[5] S. Sulaeman, M. Benidris, J. Mitra, and C. Singh, "A wind farm reliability model considering both wind variability and turbine forced outages," *IEEE Transactions on Sustainable Energy*, vol. 8, no. 2, pp. 629–637, 2017.

[6] A. Almutairi, M. H. Ahmed, and M. Salama, "Use of MCMC to incorporate a wind power model for the evaluation of generating capacity adequacy," *Electric Power Systems Research*, vol. 133, pp. 63–70, 2016.

[7] H. Yang, K. Xie, H.-M. Tai, and Y. Chai, "Wind farm layout optimization and its application to power system reliability analysis," *IEEE Trans. Power Syst.*, vol. 31, no. 3, pp. 2135–2143, 2016.

[8] H. Kim, C. Singh, and A. Sprintson, "Simulation and estimation of reliability in a wind farm considering the wake effect," *IEEE Transactions on Sustainable Energy*, vol. 3, no. 2, pp. 274–282, 2012.

[9] N. Moskalenko, K. Rudion, and A. Orths, "Study of wake effects for offshore wind farm planning," in *2010 Modern Electric Power Systems*. IEEE, 2010, pp. 1–7.

[10] J.-F. Toubeau, P.-D. Dapoz, J. Bottieau, A. Wautier, Z. De Grève, and F. Vallée, "Recalibration of recurrent neural networks for short-term wind power forecasting," *Electric Power Systems Research*, vol. 190, p. 106639, 2021.

[11] S. Li, D. C. Wunsch, E. A. O'Hair, and M. G. Giesselmann, "Using neural networks to estimate wind turbine power generation," *IEEE Trans. Energy Convers.*, vol. 16, no. 3, pp. 276–282, 2001.

[12] F. Pelletier, C. Masson, and A. Tahan, "Wind turbine power curve modelling using artificial neural network," *Renewable Energy*, vol. 89, pp. 207–214, 2016.

[13] M. Schlechtingen, I. F. Santos, and S. Achiche, "Using data-mining approaches for wind turbine power curve monitoring: a comparative study," *IEEE Transactions on Sustainable Energy*, vol. 4, no. 3, pp. 671–679, 2013.

[14] A. Clifton, L. Kilcher, J. Lundquist, and P. Fleming, "Using machine learning to predict wind turbine power output," *Environmental research letters*, vol. 8, no. 2, p. 024009, 2013.

[15] Z. Ti, X. W. Deng, and M. Zhang, "Artificial neural networks based wake model for power prediction of wind farm," *Renewable Energy*, vol. 172, pp. 618–631, 2021.

[16] NREL, "FLORIS. Version 2.2.3," 2020, Last access: January 2023. [Online]. Available: https://github.com/NREL/floris

[17] A. Niayifar and F. Porté-Agel, "Analytical modeling of wind farms: A new approach for power prediction," *Energies*, vol. 9, no. 9, p. 741, 2016.

[18] B. M. Doekemeijer, E. Simley, and P. Fleming, "Comparison of the gaussian wind farm model with historical data of three offshore wind farms," *Energies*, vol. 15, no. 6, p. 1964, 2022.

[19] H. Dong, J. Xie, and X. Zhao, "Wind farm control technologies: from classical control to reinforcement learning," *Progress in Energy*, 2022.

[20] D. R. Houck, "Review of wake management techniques for wind turbines," *Wind Energy*, vol. 25, no. 2, pp. 195–220, 2022.

[21] R. He, H. Yang, and L. Lu, "Optimal yaw strategy and fatigue analysis of wind turbines under the combined effects of wake and yaw control," *Applied Energy*, vol. 337, p. 120878, 2023.

[22] B. M. Doekemeijer, D. van der Hoek, and J.-W. van Wingerden, "Closed-loop model-based wind farm control using floris under time-varying inflow conditions," *Renewable Energy*, vol. 156, pp. 719–730, 2020.

[23] RAVE: Research at Ahlpa Ventus. Last access: January 2023. [Online]. Available: https://rave-offshore.de/en/data.html

[24] J.-A. Dahlberg, "Assessment of the lillgrund windfarm, power performance and wake effects. lillgrund pilot project," Jun 2009.

[25] Offshore wind farms in belgium. Last access: January 2023. [Online]. Available: https://odnature.naturalsciences.be/mumm/en/windfarms/

[26] H. Hersbach, B. Bell, P. Berrisford, G. Biavati, A. Horányi, J. Muñoz Sabater, J. Nicolas, C. Peubey, R. Radu, I. Rozum, D. Schepers, A. Simmons, S. C., D. Dee, and J.-N. Thépaut, "ERA5 hourly data on single levels from 1959 to present," Copernicus Climate Change Service (C3S) Climate Data Store (CDS), 2018, Last access: January 2023. [Online]. Available: 10.24381/cds.adbb2d47

[27] J.-F. Toubeau, T. Morstyn, J. Bottieau, K. Zheng, D. Apostolopoulou, Z. De Grève, Y. Wang, and F. Vallée, "Capturing spatio-temporal dependencies in the probabilistic forecasting of distribution locational marginal prices," *IEEE Transactions on Smart Grid*, vol. 12, no. 3, pp. 2663–2674, 2020.

[28] J.-F. Toubeau, J. Bottieau, F. Vallée, and Z. De Grève, "Deep learning-based multivariate probabilistic forecasting for short-term scheduling in power markets," *IEEE Trans. Power Syst.*, vol. 34, no. 2, pp. 1203–1215, 2018.

[29] F. Vallée, J. Lobry, and O. Deblecker, "System reliability assessment method for wind power integration," *IEEE Trans. Power Syst.*, vol. 23, no. 3, pp. 1288–1297, 2008.

[30] R. Billinton, H. Chen, and R. Ghajar, "Time-series models for reliability evaluation of power systems including wind energy," *Microelectronics Reliability*, vol. 36, no. 9, pp. 1253–1261, 1996.

[31] J. Carroll, A. McDonald, and D. McMillan, "Failure rate, repair time and unscheduled O&M cost analysis of offshore wind turbines," *Wind Energy*, vol. 19, no. 6, pp. 1107–1119, 2016.

[32] N. Huang, Q. Chen, G. Cai, D. Xu, L. Zhang, and W. Zhao, "Fault diagnosis of bearing in wind turbine gearbox under actual operating conditions driven by limited data with noise labels," *IEEE Transactions on Instrumentation and Measurement*, vol. 70, pp. 1–10, 2020.

[33] Y. Zhu, C. Zhu, C. Song, Y. Li, X. Chen, and B. Yong, "Improvement of reliability and wind power generation based on wind turbine real-time condition assessment," *International Journal of Electrical Power & Energy Systems*, vol. 113, pp. 344–354, 2019.

[34] Reliability Test System Task Force, "The IEEE reliability test system - 1996," *IEEE Trans. Power Syst.*, vol. 14, Aug. 1999.

[35] C. L. Archer, A. Vasel-Be-Hagh, C. Yan, S. Wu, Y. Pan, J. F. Brodie, and A. E. Maguire, "Review and evaluation of wake loss models for wind energy applications," *Applied Energy*, vol. 226, pp. 1187–1207, 2018.

[36] X. Dui, G. Zhu, and L. Yao, "Two-stage optimization of battery energy storage capacity to decrease wind power curtailment in grid-connected wind farms," *IEEE Transactions on Power Systems*, vol. 33, no. 3, pp. 3296–3305, 2017.

[37] C. Barrows, A. Bloom, A. Ehlen, J. Ikäheimo, J. Jorgenson, D. Krishnamurthy, J. Lau, B. McBennett, M. O'Connell, E. Preston *et al.*, "The IEEE reliability test system: A proposed 2019 update," *IEEE Transactions on Power Systems*, vol. 35, no. 1, pp. 119–127, 2019.